

Cross Attention-guided Dense Network for Images Fusion

Zhengwen Shen, Jun Wang*

Zaiyu Pan, Yulian Li, Jiangyu Wang

China University of Mining and Technology, Xuzhou, 221000, China

shenzw21@cumt.edu.cn, jrobot@126.com

{pzycumt, lylcumtedu, wjycumt}@163.com

Abstract

In recent years, various applications in computer vision have achieved substantial progress based on deep learning, which has been widely used for image fusion and shown to achieve adequate performance. However, suffering from limited ability in modelling the spatial correspondence of different source images, it still remains a great challenge for existing unsupervised image fusion models to extract appropriate feature and achieves adaptive and balanced fusion. In this paper, we propose a novel cross attention-guided image fusion network, which is a unified and unsupervised framework for multi-modal image fusion, multi-exposure image fusion, and multi-focus image fusion. Different from the existing self-attention module, our cross attention module focus on modelling the cross-correlation between different source images. Using the proposed cross attention module as core block, a densely connected cross attention-guided network is built to dynamically learn the spatial correspondence to derive better alignment of important details from different input images. Meanwhile, an auxiliary branch is also designed to model the long-range information, and a merging network is attached to finally reconstruct the fusion image. Extensive experiments have been carried out on publicly available datasets, and the results demonstrate that the proposed model outperforms the state-of-the-art quantitatively and qualitatively. The source code is available at <https://github.com/shenzw21/CADNIF>.

1 Introduction

Image fusion, which aims at unifying the feature information from different source images into an efficient representation and advancing the visual perception performance of humans and machines. Particularly, image fusion has a wide and various applications in computer vision, such as multi-modal image fusion: infrared and visible image fusion(Li and Wu 2018), RGB and depth image fusion for semantic segmentation(Wang et al. 2020), medical image fusion(Ma et al. 2020), etc; multi-focus image fusion(Zhang et al. 2021); multi-exposure image fusion(Ram Prabhakar, Sai Srikar, and Venkatesh Babu 2017), etc.

In recent years, traditional methods for image fusion take the lead and group three main directions: transform domain approach(Cao et al. 2014), sparse representation(Bin, Chao,

and Guoyu 2016; Zhang et al. 2018), various component analysis(Kuncheva and Faithfull 2013). While many traditional methods are proposed and perform well in image fusion task, there also exists shortcoming and limitations: the feature extraction relies on handcrafted, lack of flexibility and generalization ability. With the development and wide application of deep learning, the limitations of traditional methods got a certain breakthrough and many image fusion methods based on deep learning are proposed(Ram Prabhakar, Sai Srikar, and Venkatesh Babu 2017; Li and Wu 2018; Ma et al. 2019). Although existing methods proposed based on deep learning improve the performance and generalization ability, image fusion still suffer from feature extraction and modelling spatial correspondence learning from source images issues. For example, design fusion strategy need more artificial for different fusion tasks, the balance of feature extraction and effective jointly representation learning from source images. In order to solve the mentioned problems, in this paper we proposed a novel cross attention-guided dense network for multi-task image fusion which is constructed by cross attention-guided densenet, auxiliary network, and merging network. Modelling the cross-correlation, we proposed the cross attention-guided dense network focus on the spatial correspondence from source images by dense connected strategy. Avoiding lack of the global information, we adopted an auxiliary network for extract the long-range information. To better reconstruct the fusion image, we adopted a residual connect merging network to aggregate the fusion feature from source images.

The main contributions of this paper are summarized as follows:

- A. We propose a novel multi-task images fusion method, which is named Cross Attention-guided Dense Network for Images Fusion(CADNIF). It utilizes the advantage of the deep neural network model with attention mechanisms, and improves the ability of feature extraction and modelling spatial correspondence from source images effectively and robustness.
- B. We propose a new attention-guided dense network to modelling spatial correspondence from source images. To preserve more global information and details from source images, we employ an auxiliary network to cap-

*Corresponding author

ture long-range information and a dilated residual dense blocks with larger receptive field for reconstructing the fusion image.

- C. Extensive experiments on different datasets validate the superiority of the proposed CADNIF, which is successfully applied to multi image fusion tasks with superior performance against the state-of-the-art methods.

2 Related Work

In this section, we group the image fusion methods into two categories, traditional methods and deep learning-based approaches for image fusion. We also briefly introduce the dense block and attention mechanisms, which are highly related to our proposed method.

Image fusion. In the field of image fusion, the key to the evaluation of fusion algorithms is how to effectively extract features and fuse features. Numbers of traditional image fusion methods have been proposed to solve the feature extract problem, and group the methods into three main categories: transform domain approach, such as discrete cosine(DCT), discrete wavelet(DWT), etc; sparse representation domain approach; various component analysis, such as principal component analysis(PCA), independent component analysis(ICA), etc. However, the feature extraction methods lack flexibility and generalizability because of the increasing complexity. Moreover, traditional methods need to pay much attention to design the appropriateness of fusion methods to ensure the features come from different specific source images.

With the wide application of deep learning in high-level vision tasks, the limitations of traditional methods have a breakthrough to a certain extent. More and more CNNs based approaches were introduced for feature extraction as a backbone for image fusion tasks via various fusion strategies. The deep learning-based approaches for image fusion have been application successful in several areas, such as multi-modal image fusion, multi-exposure image fusion, multi-focus image fusion, and medical image fusion. (Ram Prabhakar, Sai Srikar, and Venkatesh Babu 2017) proposed a deep learning-based unsupervised Deepfuse framework for exposure and extreme exposure image fusion. (Li and Wu 2018) proposed an infrared and visible image fusion method named DenseFuse based on Deepfuse and incorporated dense block in the encoding network for feature extraction. (Ma et al. 2019) proposed a FusionGAN based on the generative adversarial network for infrared and visible image fusion. (Ma et al. 2020) extended previous work to adopt a dual-discriminator strategy for fusing multi-modality images of multi-resolution image fusion. Recently, some works are focus on unified unsupervised end-to-end image fusion network, (Xu et al. 2020; Zhang et al. 2020a) are each proposed unified fusion network for image fusion, such as multi-modal multi-exposure, multi-focus. However, above methods focus on significance of the difference between the different source images and do not consider the adaptability balance of the final fusion information from source images. In this paper, we propose a more generic unified unsupervised approach to multi image fusion task, which joint learn-

ing spatial correspondence information from source images, and for each cross attention module outputs, makes it possible for building a balance that each source images become one.

Image fusion with dense block. While deep convolution neural network has achieved remarkable results in the field of computer vision, with the wide application and the depth increased, gradually exposed a lot of problems, such as performance degradation, vanishing gradient, exploding gradient, and previous features not reused fully, etc. To address the above problems, (He et al. 2016) proposed a deep residual learning network, based on He’s work, (Huang et al. 2017) proposed a new network framework densenet, which each layers can be concatenated by previous layer and as an input for the next layer and strengthen feature propagation, encourage feature reuse, and alleviates the problem of the gradient. Based on the above advantages, the dense block has been widely incorporated into multi computer vision tasks, such as semantic segmentation, image classification, object detection, etc. In the image fusion task, a dense block is widely used in feature extraction. (Li and Wu 2018) incorporate the dense block into the encoding network, preserve the useful information from middle layers. (Ma et al. 2020) proposed a novel GAN framework for image fusion and the architecture of the generator is based on densenet. Instead of directly using densenet as a feature extraction network, we propose cross attention-guided dense network, which effective learning cross-correlation information between different source images.

Attention mechanisms in deep learning methods. In recent years, with the emergence of attention mechanism, which is a technique that enables models to focus on important information and fully learn to absorb it, it has been widely used in many computer vision tasks, natural language processing, image and video understanding. (Bastidas and Tang 2019) proposed a novel channel attention network for multi-spectral imagery. (Tian, Guo, and Long 2021) proposed a multi-level attention to address the problem of Crowd Counting. (Song et al. 2021) proposed a cross-modal attention for MRI and Ultrasound Volume Registration. Our work explores cross attention for basic mutual feature extraction of source images.

3 Methods

We propose a novel cross attention-guided image fusion framework, which focuses on improving the cross significance information representation, modelling the spatial correspondence, capture the long-range information and merging the feature from source images to reconstruct the fusion image. As shown in Figure 1, there are three networks: cross attention-guided dense network, auxiliary network, and merging networks. The attention-guided network captures the spatial correspondence feature via using five attention blocks based on densenet, the responsible of auxiliary for capture the long-range information, while the merging network relying on a series of dilated residual dense blocks to utilize the image features effectively and obtain the fusion images more details. Finally, the proposed attention-guided

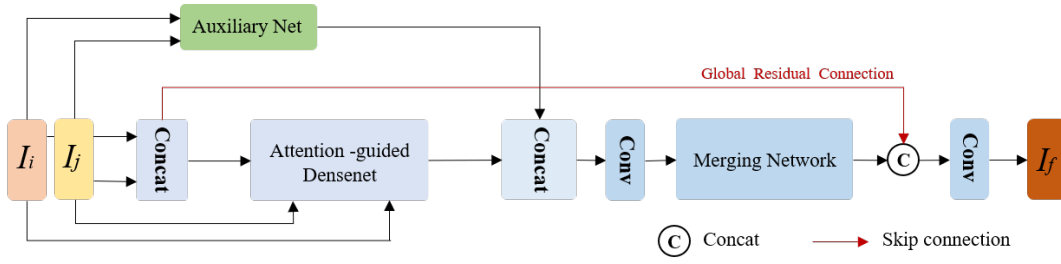


Figure 1: The overall architecture of the proposed CADNIF mainly consists of three components: Attention-guided Network, Auxiliary network, and Merging Network. Firstly, the attention-guided network is adopted to extract cross attention feature from source images. Simultaneously, the auxiliary network extracts the long-range feature representations via series convolution. Finally, merging network merging the global feature representations and the spatial correspondence via a dilated residual dense block and global residual connection.

fusion network further to fuse the source images and the following experiments show that the fusion result prefers well.

3.1 Cross Attention Guided Densenet

Unlike the previous methods, which use the densenet as a feature extract network directly, our proposed cross attention guided densenet obtains the cross-attention information from each source image. As shown in Figure 2, the attention-guided densenet consists of five major cross attention blocks. Given input images I_i and I_j , each input image is concatenated by three one-channel gray images of the same source. We first concatenate the input images and obtain the 6-channel concatenation image. As shown in Figure 2a, the input images and the concatenated image feed into the attention-guided network, and obtain the final cross attention features via dense connection. As shown in Figure 2b, the cross attention guided block consists of three convolution layers to obtain feature maps, concatenate operation, and attention module. Details of the cross attention block are provided below. The final cross attention maps can be obtained via:

$$A_i = \text{Attent}(I_i, \text{Concat}(I_i, I_j)) \quad (1)$$

$$A_j = \text{Attent}(I_j, \text{Concat}(I_i, I_j)) \quad (2)$$

$$Z_g = \text{Concat}(\text{Concat}(I_i, I_j), A_i \circ I_i, A_j \circ I_j) \quad (3)$$

where \circ denotes the point-wise multiplication, I_i and I_j denote the original input images, Z_i and Z_j denote each original image concatenate with $\text{Concat}(I_i, I_j)$, A_i and A_j denote the attention map, Z_g denote the final cross attention feature maps.

3.2 Attention Module

Attention modules play an important role in the cross attention block, as shown in Figure 2c, to obtain the one-to-one correspondence maps for each source image, the attention module consists of two convolution layers and a Sigmoid layer. From Eq. 3, the input of the attention module is A_i or A_j , and obtain the feature maps via two convolution layers. Each convolution layer applies 3×3 layers. Respectively, a ReLU activation and a Sigmoid activation in the module after convolution operation. As a result, we finally obtain the attention map Z_g with values in the range $[0, 1]$.

3.3 Auxiliary network

As shown in Figure 3, in the auxiliary network, we first use 1×1 convolution kernel to obtain 32-channels feature maps via concatenating operation of the input images I_i and I_j , then we use a convolution block consists of three different kernel size convolution operation branches, 1×1 , 3×3 , 5×5 , respectively, each of convolutions is followed by layer normalization. Finally, obtain the final fusion feature maps via concatenate operation and followed a layer normalization after the convolution of 1×1 kernel.

3.4 Merging Network

To better reconstruct the fused image, integrate the cross-correlation information and long-range information to obtain more details of the feature maps, we adopt a dilated residual dense block proposed in (Yan et al. 2019) as the reconstructed network. The merging network takes the concatenated feature maps after a convolution layer of 1×1 kernel operation as input, which is concatenated from the attention-guided network and auxiliary network. As shown in figure 4, the dilated residual dense block consists of three convolution layers followed by ReLU activation, concatenation-based skip-connection similar to densenet, and a convolution layer of 1×1 kernel operation as output. Different from the normal convolution operation, each convolution layers adopt 2-dilated convolutions, kernel size is 3×3 . Finally, we apply a global residual connection strategy to concatenate the output with concatenation image from source images.

3.5 Training Loss

As described above section, the proposed CANIF method can be trained to obtain the context details structural and the background details from the different sources images. In the proposed method, the loss function consists of Mean Square Error(MSE) loss L_{mse} and Structural Similarity(SSIM) loss L_{ssim} . The SSIM loss is an index to measure the similarity of two images, the larger the value, the better, the maximum is 1. Generally, if the value is 1, then the fused image retains the input images more structural details, the L_{ssim} is

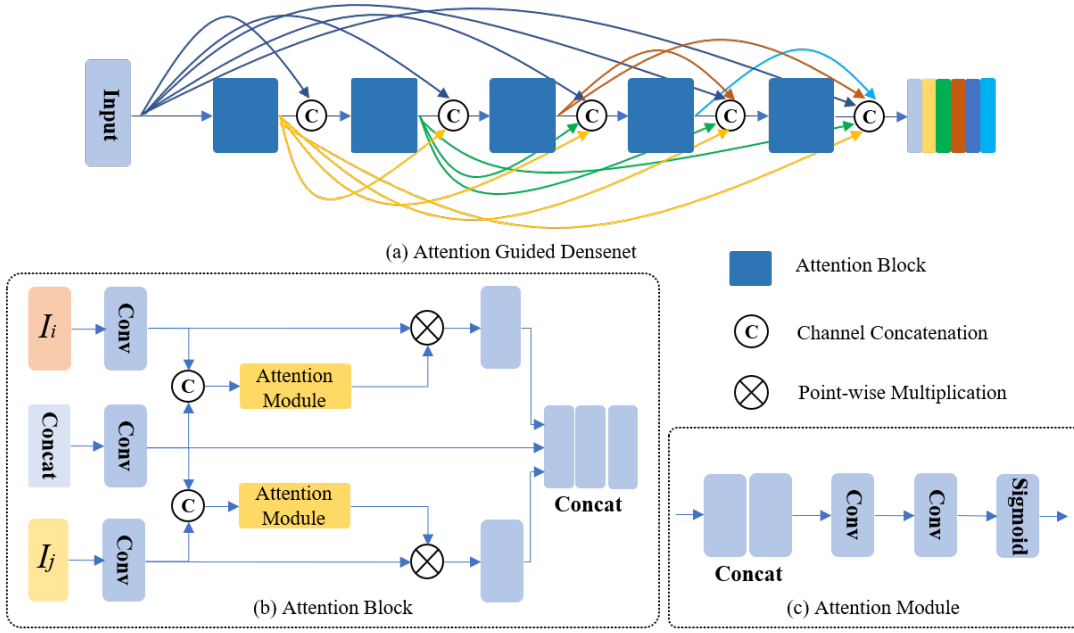


Figure 2: (a) The architecture of the proposed attention-guided dense network, the network consists of five attention blocks for modelling the spatial correspondence. (b) shows the cross attention blocks. (c) shows the attention module.

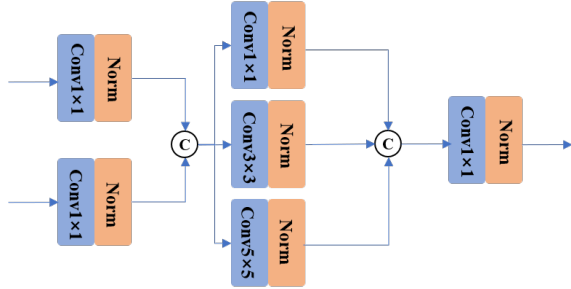


Figure 3: The architecture of the auxiliary network.

defined by Eq. 4,

$$L_{ssim} = 1 - SSIM(O, I) \quad (4)$$

where I denotes the input source image, O denotes the fused image, $SSIM(\cdot)$ denotes the measures structural similarity. The MSE loss emphasize the matching of each corresponding pixel between the input image and output image, the MSE loss L_{mse} is calculated as Eq. 5,

$$L_{mse} = \|I_f - I\|_2^2 \quad (5)$$

where I denotes the input source image, I_f denotes the fused image, $\|\cdot\|_2^2$ denotes the l_2 normal. Finally, the total losses L_{total} of the proposed model can be expressed as follows:

$$L_{total} = \lambda_{mi} I_{mse_i} + \lambda_{mj} I_{mse_j} + \lambda_{si} I_{ssim_i} + \lambda_{sj} I_{ssim_j} \quad (6)$$

where $\lambda_{(\cdot)}$ denotes the contribution of each loss to the whole objective function. In this paper, for each experiment below, setting the parameter λ_{mi} , λ_{mj} , λ_{si} , λ_{sj} equal to: 1,

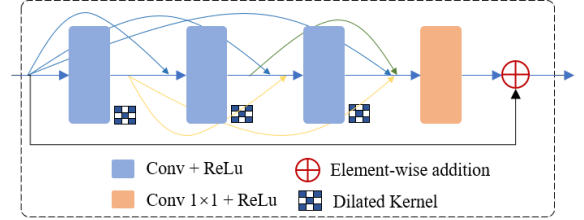


Figure 4: The detail architecture of the merging network.

0.5, 0.03, 0.03, in infrared and visible fusion experiment; 1, 1, 0.01, 0, in MRI and PET fusion experiment; 2, 5, 1, 1, in Multi-focus fusion experiment; 0.5, 0.7, 1.3, 1, in Multi-exposure fusion experiment.

4 Experiments

To demonstrate the proposed method, we conduct the experiments on five publicly available datasets: TNO¹ and RoadScene² datasets for visible and infrared image fusion task, TNO used for training, RoadScene are all used for testing; MFF and SICE datasets³ for multi-exposure image fusion task; MRI and PET⁴ datasets for medical image fusion task; Lytro⁵ for multi-focus image fusion task. For the lack of training data problem, we adopt the expansion strategy

¹<http://figshare.com/articles/TNOImageFusionDataset/1008029>

²<https://github.com/hanna-xu/RoadScene>

³<https://drive.google.com/drive/folders>

⁴<http://www.med.harvard.edu/AANLIB/home.html>

⁵<https://github.com/sametaymaz/Multi-focus-Image-Fusion-Dataset>

Methods	EN	SCD	SD	Qabf	MI
CE	7.1939	1.5846	90.6729	0.4798	14.3879
DDLatLRR	6.8565	1.7255	76.3305	0.4881	13.7131
DenseFuse	6.8425	1.6183	89.3237	0.5350	13.6851
PMGI	7.1191	0.1062	99.6564	0.1535	14.1382
U2Fusion	6.8959	1.5877	76.4380	0.3941	13.7919
Proposed	7.2841	1.8318	104.3948	0.3256	14.5683

Table 1: Quantitative evaluation for each methods via 17 pairs infrared and visible image fusion of TNO dataset.

based on(Zhang et al. 2020a). For the testing, the number of image pairs used for testing dataset is 17, 50, 19, 20, and 18, respectively.

For all experiments, we set the batchsize, learning rate, and epoch equal to 16, 10^{-5} , 10, respectively. The proposed method was implemented on NVIDIA GEFORCE RTX 2080 Ti GPU and based on TensorFlow.

4.1 Infrared and visible image fusion

In the infrared and visible image fusion experiment, most TNO datasets are used to train the proposed image fusion method, image pairs used for testing is 17, and 50 pairs of RoadSence datasets are used to test our proposed method to verify its generalization and model robustness. We compare our proposed method with CE(Zhou et al. 2016), DDLatLRR(Li, Wu, and Kittler 2020), DenseFuse(Li and Wu 2018), PMGI(Zhang et al. 2020a), U2Fusion(Xu et al. 2020).

To effective quantitatively evaluate the fusion quality, we adopt five related indicators to compare the existing methods, namely entropy (EN), sum of the correlations of differences (SCD)(Aslantas and Bendes 2015), standard deviation (SD), represents the ratio of noise added to the final image(Qabf), and mutual information (MI). As shown in Table 1 and Table 2, the quantitative result of TNO and RoadSence dataset, the red font in italic represents the best value and the bold black font in italic represents the second best value. Similarly, we can infer that the quantitative value of proposed method outperform in EN, SCD, SD and MI metrics. It demonstrates that the proposed method maintains abundant correspondence spatial information and detail information from source images.

The qualitative fusion results on two typical image pairs of each test dataset are illustrated Figure 5 and Figure 6, red box highlights are the local fine features. From the results of TNO dataset and RoadSence dataset, we can observe that the proposed method capture abundant correspondence semantic information compare with the state-of-the-art methods. Similarly, the highlights information obtained by zooming in on local fine features, we can infer that the local fine information retained well from source images, such as sky, window, license plate, and the top of the tree, etc. In particular, for each source image illumination information and texture details, the fusion result shows that the proposed method performs well by adaptive balance strategy via cross attention-guided network.

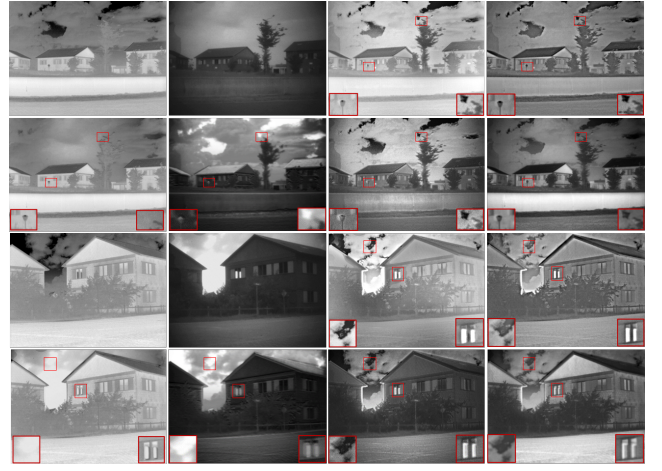


Figure 5: Comparison result of infrared and visible image fusion of TNO datasets. From left to right: infrared image, visible image, the results of CE, DDLatLRR, DenseFuse, PMGI, U2Fusion and proposed.

Methods	EN	SCD	SD	Qabf	MI
CE	7.3635	1.5893	75.8509	0.4587	14.7271
DDLatLRR	7.1485	1.6482	67.6889	0.5017	14.2971
DenseFuse	6.8549	1.2950	65.5098	0.5074	13.7099
PMGI	7.2492	1.7410	78.2691	0.4230	14.6985
U2Fusion	7.1968	1.7692	68.0393	0.4791	14.3937
Proposed	7.5315	1.7785	97.9758	0.4571	15.0631

Table 2: Quantitative evaluation for each methods via 50 pairs infrared and visible image fusion of RoadSence dataset.

4.2 MRI and PET image fusion

In the MRI and PET image fusion experiment, the number of test image pairs is 20. We compare our proposed method with DCHWT(Kumar 2013), Structure Aware(Li et al. 2018), DDCTPCA(Naidu 2014), PMGI(Zhang et al. 2020a), IFCNN(Zhang et al. 2020b) by quantitative and qualitative evaluation metrics.

We adopt five related indicators to compare the existing methods, namely entropy (EN), Feature mutual information (FMI), standard deviation (SD), represents the ratio of noise added to the final image(Qabf), and mutual information (MI). As shown in Table 3, we can observe that the proposed fusion method outperforms in CC, and MI metrics, in EN metric, the result performance better than other methods but DCHWT. Qualitative results can be seen from Figure 7, the spatial correspondence details information is preserved, and the local context detail information is contained from source input images.

4.3 Multi-focus Image Fusion

To verify the proposed method ability which extract features, versatility, and generalization from source images, we conducted fusion experiments based on the near-focused and far-focused image datasets. At the same time, our proposed method was compared with other methods, which



Figure 6: Comparison result of infrared and visible image fusion of RoadSense datasets. From left to right: infrared image, visible image, the results of CE, DDLatLRR, DenseFuse, PMGI, U2Fusion and proposed.

Methods	EN	SD	CC	Qabf	MI
DCHWT	5.7501	84.9344	0.7302	0.6849	11.1003
SA	4.9705	84.6888	0.7079	0.7415	9.9411
DDCTPCA	4.8017	84.9032	0.8030	0.4486	9.6035
PMGI	5.3341	83.9781	0.7646	0.6917	10.6684
IFCNN	4.8187	98.1931	0.7726	0.6662	9.6374
Proposed	5.5149	80.2054	0.8180	0.6211	11.1298

Table 3: Quantitative evaluation for each methods via 20 pairs of MRI and PET image fusion.

specialized focused on the far and near focused images fusion task. We employ five existing methods to compare with our method: VSMWLS(Ma et al. 2017), CBF(Kumar 2015), Structure Aware(Li et al. 2018), ConvSR(Liu et al. 2016) and MFF(Zhang et al. 2021), respectively.

For quantitative analysis, we adopt five related indicators to compare the existing methods, namely entropy (EN), feature mutual information (FMI), standard deviation (SD), mutual information (MI), and correlation coefficient (CC). As shown in Table 4, we can infer that the proposed fusion method outperform in SD metric, outperform in EN, MI, and CC metrics but MFF and VSMWLS method. More intuitively for qualitative analysis, from Figure 8, it demonstrates that our proposed method has a good feature extraction capability of illumination information and spatial details information for multi-focus images compared with the specialized methods.

4.4 Multi-exposure Image Fusion

In the multi-exposure image fusion experiment, we employ five existing methods to compare with our method: FMMR(Li and Kang 2012), DSIFT(Hayat and Imran 2019), DeepFuse(Ram Prabhakar, Sai Srikar, and Venkatesh Babu 2017), MGFF(Bavirisetti et al. 2019) and IFCNN(Zhang et al. 2020b), respectively.

From Table 5, compare the five existing methods by en-

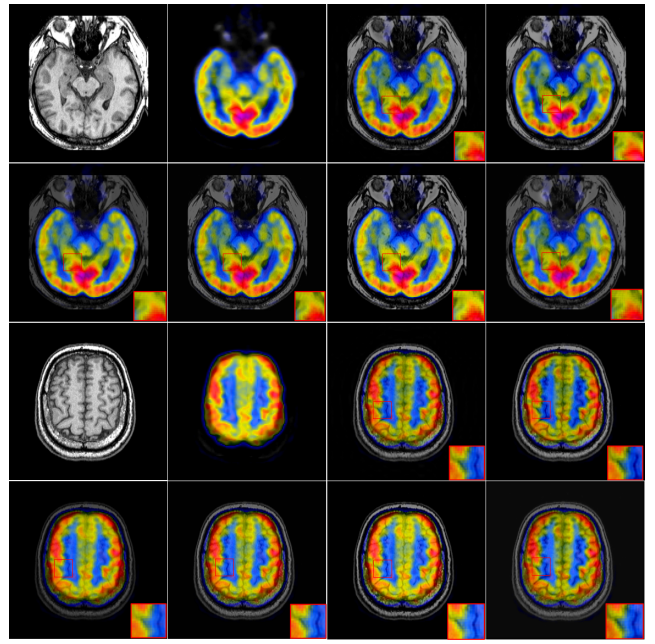


Figure 7: Comparison result of MRI and PET image fusion. From left to right: MRI image, PET image, the results of DCHWT, Structure Aware(SA), DDCTPCA, PMGI, IFCNN and Proposed.

Methods	EN	FMI	SD	MI	CC
VSMWLS	7.4934	0.8850	106.0445	15.0068	0.9564
CBF	7.4699	0.8927	106.5535	14.9399	0.9514
SA	7.3825	0.8943	107.3123	14.7652	0.9495
ConvSR	7.4615	0.8940	107.3435	14.9230	0.9496
MFF	7.5666	0.8826	111.8743	15.1333	0.9515
Proposed	7.5005	0.8788	113.1872	15.0811	0.9530

Table 4: Quantitative evaluation for each specialized methods via 18 pairs of Far-focused and Near-focused image fusion.

trophy (EN), Feature mutual information (FMI), standard deviation (SD), correlation coefficient (CC), and mutual information (MI). We can observe that the proposed fusion method outperforms in SD and CC metrics, in EN and MI metric our method outperforms but MGFF and DeepFuse. Visual comparison results of each image fusion method can be seen from Figure 9. From the perspective of global image information, the proposed method adaptive balance the illuminate information well, similarly the local context detail information is retained and presented from source images.

4.5 Ablation Study and Visualization

In this section, we take an ablation study which is conducted on infrared and visible images fusion experiment as an example. Compared with dilated residual dense block(DRDB) and original densenet without cross attention-guided module. As shown in Table 6, the bold black font in italic represents the best value. It is evident that for the reconstructed fusion image, the proposed method can effect modelling the

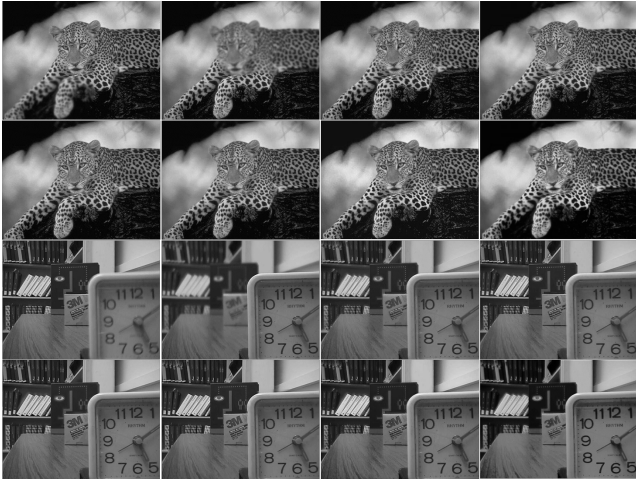


Figure 8: Comparison result of Multi-focus image fusion. From left to right: Far-focused, Near-focused, the results of VSMWLS, CBF, Structure Aware, ConvSR, MFF and Proposed.

Methods	EN	FMI	SD	CC	MI
FMMR	6.3172	0.8736	92.5337	0.5448	12.6344
DISIFT	6.5245	0.8934	101.3824	0.5445	13.0491
DeepFuse	6.8183	0.8926	116.3688	0.7945	13.8566
MGFF	6.8792	0.8874	116.2462	0.7976	13.7586
IFCNN	6.7259	0.8838	113.8987	0.7572	13.4519
Proposed	6.8598	0.8619	122.6287	0.8202	13.8398

Table 5: Quantitative comparisons of the 19 pairs of underexposed and overexposed image by five metrics.

spatial correspondence, and the DRDB module can obtain sufficient information from the reconstructed image based on a multi-illumination image by use dilated convolution to obtain a larger receptive field to generate illusion and details.

As shown in Figure 10, we visualize the cross attention maps obtained by each cross-attention module. Taking infrared and visible image fusion task as an example, we can infer from the figure that the fusion image background, detail information, and significance features obtained by each attention module are enhanced. It shows that the cross attention-guided is effective for the extraction of spatial correspondence feature information from source images.

5 Conclusion

This work introduced a novel unsupervised framework for the challenging multi-image fusion task, and it can serve as a unified framework for four tasks including infrared and visual image fusion, medical image fusion, multi-focus image fusion, and multi-exposure image fusion. To learn semantic features better for image fusion effectively, a cross attention-guided dense network is proposed to learn the spatial correspondence explicitly, and only the essential details are then learned and aligned attentively. We also proposed an auxiliary branch and a global merging block to better model the long-range relationship and better leverage the global infor-



Figure 9: Comparison result of Multi-exposure image fusion. From left to right: underexposed image, overexposed image, the fusion results of FMMR, DISIFT, DeepFuse, MGFF, IFCNN and Proposed.

Methods	EN	SCD	SD	Qabf	MI
Densenet	7.0573	0.5774	100.39	0.3050	14.1147
Without DRDB	7.1020	1.3297	97.9295	0.2757	14.2040
Proposed	7.2841	1.8318	104.3948	0.3256	14.5683

Table 6: Ablation Study on cross attention-guided network for infrared and visible image fusion.



Figure 10: The attention map of cross attention unit from the source images.

mation to reconstruct the fused image. Through quantitative comparison and qualitative analysis, the proposed method achieves better result compared with the state-of-the-art fusion methods.

6 Acknowledgments

This work was partially supported by the Scientific Innovation 2030 Major Project for New Generation of AI under Grant 2020AAA0107300.

References

- Aslantas, V.; and Bendes, E. 2015. A new image quality metric for image fusion: the sum of the correlations of differences. *Aeu-international Journal of electronics and communications*, 69(12): 1890–1896.
- Bastidas, A. A.; and Tang, H. 2019. Channel Attention Networks. In *2019 IEEE/CVF Conference on Computer Vision and Pattern Recognition Workshops (CVPRW)*, 881–888.
- Bavirisetti, D. P.; Xiao, G.; Zhao, J.; Dhuli, R.; and Liu, G. 2019. Multi-scale guided image and video fusion: A fast and

- efficient approach. *Circuits, Systems, and Signal Processing*, 38(12): 5576–5605.
- Bin, Y.; Chao, Y.; and Guoyu, H. 2016. Efficient image fusion with approximate sparse representation. *International Journal of Wavelets, Multiresolution and Information Processing*, 14(04): 1650024.
- Cao, L.; Jin, L.; Tao, H.; Li, G.; Zhuang, Z.; and Zhang, Y. 2014. Multi-focus image fusion based on spatial frequency in discrete cosine transform domain. *IEEE signal processing letters*, 22(2): 220–224.
- Hayat, N.; and Imran, M. 2019. Ghost-free multi exposure image fusion technique using dense SIFT descriptor and guided filter. *Journal of Visual Communication and Image Representation*, 62: 295–308.
- He, K.; Zhang, X.; Ren, S.; and Sun, J. 2016. Deep residual learning for image recognition. In *Proceedings of the IEEE conference on computer vision and pattern recognition*, 770–778.
- Huang, G.; Liu, Z.; Van Der Maaten, L.; and Weinberger, K. Q. 2017. Densely connected convolutional networks. In *Proceedings of the IEEE conference on computer vision and pattern recognition*, 4700–4708.
- Kumar, B. S. 2013. Multifocus and multispectral image fusion based on pixel significance using discrete cosine harmonic wavelet transform. *Signal, Image and Video Processing*, 7(6): 1125–1143.
- Kumar, B. S. 2015. Image fusion based on pixel significance using cross bilateral filter. *Signal, image and video processing*, 9(5): 1193–1204.
- Kuncheva, L. I.; and Faithfull, W. J. 2013. PCA feature extraction for change detection in multidimensional unlabeled data. *IEEE transactions on neural networks and learning systems*, 25(1): 69–80.
- Li, H.; and Wu, X.-J. 2018. DenseFuse: A fusion approach to infrared and visible images. *IEEE Transactions on Image Processing*, 28(5): 2614–2623.
- Li, H.; Wu, X.-J.; and Kittler, J. 2020. MDLatLRR: A novel decomposition method for infrared and visible image fusion. *IEEE Transactions on Image Processing*. Doi: 10.1109/TIP.2020.2975984.
- Li, S.; and Kang, X. 2012. Fast multi-exposure image fusion with median filter and recursive filter. *IEEE Transactions on Consumer Electronics*, 58(2): 626–632.
- Li, W.; Xie, Y.; Zhou, H.; Han, Y.; and Zhan, K. 2018. Structure-aware image fusion. *Optik*, 172: 1–11.
- Liu, Y.; Chen, X.; Ward, R. K.; and Wang, Z. J. 2016. Image fusion with convolutional sparse representation. *IEEE signal processing letters*, 23(12): 1882–1886.
- Ma, J.; Xu, H.; Jiang, J.; Mei, X.; and Zhang, X.-P. 2020. DDcGAN: A dual-discriminator conditional generative adversarial network for multi-resolution image fusion. *IEEE Transactions on Image Processing*, 29: 4980–4995.
- Ma, J.; Yu, W.; Liang, P.; Li, C.; and Jiang, J. 2019. FusionGAN: A generative adversarial network for infrared and visible image fusion. *Information Fusion*, 48: 11–26.
- Ma, J.; Zhou, Z.; Wang, B.; and Zong, H. 2017. Infrared and visible image fusion based on visual saliency map and weighted least square optimization. *Infrared Physics & Technology*, 82: 8–17.
- Naidu, V. 2014. Hybrid DDCT-PCA based multi sensor image fusion. *Journal of Optics*, 43(1): 48–61.
- Ram Prabhakar, K.; Sai Srikar, V.; and Venkatesh Babu, R. 2017. Deepfuse: A deep unsupervised approach for exposure fusion with extreme exposure image pairs. In *Proceedings of the IEEE international conference on computer vision*, 4714–4722.
- Song, X.; Guo, H.; Xu, X.; Chao, H.; Xu, S.; Turkbey, B.; Wood, B. J.; Wang, G.; and Yan, P. 2021. Cross-modal Attention for MRI and Ultrasound Volume Registration. *arXiv preprint arXiv:2107.04548*.
- Tian, M.; Guo, H.; and Long, C. 2021. Multi-Level Attentive Convolutional Neural Network for Crowd Counting. *arXiv preprint arXiv:2105.11422*.
- Wang, Y.; Huang, W.; Sun, F.; Xu, T.; Rong, Y.; and Huang, J. 2020. Deep multimodal fusion by channel exchanging. *Advances in Neural Information Processing Systems*, 33.
- Xu, H.; Ma, J.; Jiang, J.; Guo, X.; and Ling, H. 2020. U2Fusion: A unified unsupervised image fusion network. *IEEE Transactions on Pattern Analysis and Machine Intelligence*.
- Yan, Q.; Gong, D.; Shi, Q.; Hengel, A. v. d.; Shen, C.; Reid, I.; and Zhang, Y. 2019. Attention-guided network for ghost-free high dynamic range imaging. In *Proceedings of the IEEE/CVF Conference on Computer Vision and Pattern Recognition*, 1751–1760.
- Zhang, H.; Le, Z.; Shao, Z.; Xu, H.; and Ma, J. 2021. MFF-GAN: An unsupervised generative adversarial network with adaptive and gradient joint constraints for multi-focus image fusion. *Information Fusion*, 66: 40–53.
- Zhang, H.; Xu, H.; Xiao, Y.; Guo, X.; and Ma, J. 2020a. Rethinking the image fusion: A fast unified image fusion network based on proportional maintenance of gradient and intensity. In *Proceedings of the AAAI Conference on Artificial Intelligence*, 12797–12804.
- Zhang, Q.; Liu, Y.; Blum, R. S.; Han, J.; and Tao, D. 2018. Sparse representation based multi-sensor image fusion for multi-focus and multi-modality images: A review. *Information Fusion*, 40: 57–75.
- Zhang, Y.; Liu, Y.; Sun, P.; Yan, H.; Zhao, X.; and Zhang, L. 2020b. IFCNN: A general image fusion framework based on convolutional neural network. *Information Fusion*, 54: 99–118.
- Zhou, Z.; Dong, M.; Xie, X.; and Gao, Z. 2016. Fusion of infrared and visible images for night-vision context enhancement. *Applied optics*, 55(23): 6480–6490.